Energy, Mines and Resources Canada | Énergie, Mines et Ressources Canada

CANMET

Canada Centre for Mineral and Energy Technology | Centre canadien de la technologie des minéraux et de l'énergie

TRIAXIAL PROPERTIES OF INDIANA LIMESTONE

M. Bétournay and T. Shimotani
Rock Mechanics Laboratory

November 1983

This document is an unedited interim report prepared primarily for discussion and internal reporting purposes. It does not represent the opinion of the Centre or its policy in this matter. (CANMET)

Ce document est un rapport provisoire non-révisé et rédigé principalement pour fin de discussion et de documentation interne. Il ne représente nulle-ment l'expression définitive de l'opinion du Centre canadien de la technologie des minéraux et de l'énergie (CANMET)

MICROMEDIA SEP 24 19[illegible]

42 pp

MINERAL RESEARCH PROGRAM
MINING RESEARCH LABORATORIES
DIVISION REPORT ERP/MRL 83-99(TR)

TRIAXIAL PROPERTIES OF INDIANA LIMESTONE

by

M. Bétournay* and T. Shimotani**

ABSTRACT

Indiana limestone, a fossiliferous oolitic limestone, was tested at CANMET to verify the validity and accuracy of the multiple failure state and strain-controlled triaxial tests. The post-peak behaviour of this rock type was examined to characterize it according to the level of brittleness ("Class I" or "Class II"). Using a stiff triaxial assembly it was found that the peak strength and accompanying strain was very similar for both tests; also that using a-priori knowledge about the stress-strain slope p to follow in obtaining the limit strength (σ_1-σ_3) curve or using the modulus of elasticity as an approximation, works. Where the p value remains essentially the same during one test, it is easy to translate the difference between approximation and true p value to the results of the obtained limit strength curve. However, because this rock type reaches the brittle-ductile transition at low confinement, σ_1 = 168 MPa, σ_3 = 46.5 MPa, the p value decreases during a test, making corrections to approximations difficult. It is felt that both the multiple failure state and strain controlled tests are valid and accurate for Indiana limestone, a rock type that exhibits "Class I" or less brittle behaviour. Hoek and Brown's empirical relationship for failure of intact and discontinuous rock is representative of the results obtained for multiple failure state or conventional triaxial tests performed on Indiana limestone.

---

*Physical Scientist, Rock Mechanics Laboratory, Mining Research Laboratories, CANMET, Energy, Mines and Resources Canada.

**Post-Doctorate Fellow (University of Tokyo), Rock Mechanics Laboratory, Mining Research Laboratories, CANMET, Energy, Mines and Resources Canada.

CARACTÉRISTIQUES TRIAXIALES DU CALCAIRE INDIANA

par

M. Bétournay* et T. Shimotani**

RÉSUMÉ

Le calcaire Indiana, un calcaire oolitique fossilifère, fut soumis à des essais triaxiaux avec états de rupture multiples et des essais de déformation imposée, dans le but de vérifier la validité et l'exactitude de ceux-ci. On a examiné le comportement de ce type de roche au delà de la résistance maximale pour le caractériser suivant son degré de fragilité ("classe I ou classe II"). En utilisant un assemblage triaxial rigide, on a constaté qu'entre ces deux essais il existaient une grande ressemblance de la résistance maximale et de la déformation l'accompagnante; on a également constaté qu'utiliser à-priori des connaissances sur la pente de la courbe contraintes-déformations p à suivre pour obtenir la courbe de résistance limite (σ_1-σ_3), ou bien d'utiliser le module d'élasticité comme valeur p, est une méthode valable. Là où la valeur p reste essentiellement fixe durant l'essai, il est facile de traduire la différence entre approximation et valeur exacte au niveau de la courbe de résistance limite. Toutefois, parce que ce type de roche atteint l'état transitionnel entre la fragilité et la ductilité à basses contraintes triaxiales (σ_1 = 168 MPa, σ_3 = 46,5 MPa) la valeur p décroit constamment pendant l'essai, ce qui rend difficile les corrections à apporter aux résultats utilisant une valeur approximative de p. On estime que les essais triaxiaux avec états de rupture multiples et les essais de déformation imposée sont valides et exacts dans le cas du calcaire Indiana, type de roche

---

*Chercheur scientifique, Laboratoire de la mécanique des roches, Laboratoires de recherche minière, CANMET, Énergie, Mines et Ressources Canada.

**Boursier au niveau post-doctoral, Laboratoire de la mécanique des roches, Laboratoires de recherche minière, CANMET, Énergie, Mines et Ressources Canada.

qui manifeste un comportement de classe "I" ou de moindre fragilité. La relation empirique de Hoek et Brown concernant la rupture des roches intactes et des roches avec discontinuités est représentative des résultats obtenus lors des essais triaxiaux avec états de rupture multiples ou des essais triaxiaux conventionnels, utilisants le calcaire Indiana.

CONTENTS

	Page
ABSTRACT	i
RÉSUMÉ	ii
INTRODUCTION	1
SPECIMEN DESCRIPTION	1
EXPERIMENTAL SET-UP	2
THEORETICAL CONSIDERATIONS	3
Multiple Failure State Test	3
Strain Controlled Triaxial Test	4
RESULTS	5
Multiple Failure State Test	5
Strain Controlled Test	10
Test Results	10
Comparison of Indiana Limestone Types	11
Specimen Behaviour	12
Hoek and Brown Failure Criteria	12
Brittle-ductile Transition	13
CONCLUSIONS	13
ACKNOWLEDGEMENTS	14
REFERENCES	15
APPENDIX 1	32
APPENDIX 2	33
APPENDIX 3	34
APPENDIX 4	35

TABLES

No.		
1.	Comparison of tested Indiana limestone	2
2.	Conventional triaxial test results	6
3.	Multiple failure state test results	7

TABLES (Cont'd)

No.		Page
4.	Comparison of theoretical and measured failure properties for conventional and multiple failure state tests	8
5.	Prediction of departure from limit strength curve for p = E = 27.5 GPa	11

FIGURES

1.	Triaxial stiff testing assembly	16
2.	Details of the Hoek triaxial pressure vessel	17
3.	Sample behaviour at peak compressive strength with varying confining pressure (after Kovari and Tisa, 1975)	18
4.	Sample behaviour at residual compressive strength with varying confining pressure (after Kovari and Tisa, 1975)	18
5.	Strain-controlled triaxial compressive tests with overestimation, proper estimation and under estimation of slope p (after Kovari et al 1983)	19
6.	Conventional triaxial compressive test results of Indiana limestone (using averages)	20
7.	Multiple failure state compressive test results of Indiana limestone (using averages)	21
8.	Stress-strain slope p of peak compressive strengths, conventional triaxial tests (using averages)	22
9.	Stress-strain slope p of peak compressive strengths, multiple failure state test (using averages)	23
10.	Mohr's peak stress envelope for theoretical and measured failure planes	24
11.	Limit strength curve for peak strength, conventional and multiple failure state compressive tests	25
12.	Limit strength curve for residual strength, conventional and multiple failure state compressive tests	26

FIGURES (Cont'd)

No.		Page
13.	Strain-controlled triaxial compressive test result, p = 15 GPa	27
14.	Strain-controlled triaxial compressive test result, p = 17.5 GPa ..	28
15.	Strain-controlled triaxial compressive test result, p = 19 GPa	29
16.	Strain-controlled triaxial compressive test result, p = 23 GPa	30
17.	Strain-controlled triaxial compressive test result, p = 27.5 GPa ..	31

INTRODUCTION

Complete testing of intact rock with a view to direct application of rock mechanics to design and safety of engineering projects is now possible with few specimens. As developed by Kovari and Tisa (1) and Kovari et al. (2), a high degree of accuracy accompanies the multiple failure state and strain-controlled triaxial tests. In the former, the specimen is brought to successive failure points, at chosen confining pressures, at or just prior to reaching peak strength. In the latter, after a first peak strength level is reached, the sample is kept in a continuous failure state by increasing the confining pressure steadily, forcing the sample to follow the stress-strain slope containing the failure points of the rock type; the limit strength curve of axial stress and confining pressure is thus obtained.

The premises of experimental validity and accuracy of these two procedures have already been demonstrated for the case of a brittle [Class II behaviour, Wawersik (3)] rock type by Shimotani (4). It is endeavored in this report to examine the results of Indiana limestone subjected to these tests, determination of rock behaviour (Class I or II) and verification of the above premises. Empirical relationships for failure of rock specimens, developed by Hoek and Brown (5) will also be established.

SPECIMEN DESCRIPTION

A 1 m by 1 m, 23 cm thick slab of Indiana limestone, obtained directly from the quarry, was used as the source of the cylindrical specimens tested. "BX" size core was diamond drilled parallel to the smallest block dimension.

The soft and chipping nature of the rock did not permit use of the roller lapper to smooth the sample to true cylindrical shape; the ends were smoothed and made parallel with a double lapper. Both lappers were developed at CANMET by B. Gorski (6).

The cylindrical specimens averaged 8.2 cm long, 4.1 cm in diameter, resulting in a 2:1 length to diameter ratio. The specimens met the ASTM* tolerances:

---

*American Society for Testing and Materials

1. ends parallel to within 0.025 mm
2. ends square to sides within 0.025 mm.

The faint bedding trace, existing parallel to the square dimensions, is orthogonal to the cylinder axis; the axial stress is thus applied perpendicular to "bedding".

The Indiana limestone tested at CANMET consists of a moderately-cemented ooid and fossil mass (pelecypods, gastropods, bryozoans), buff coloured, roughly falling under the term "oolitic" limestone. The porosity, using the mercury porosimeter is 12.96%, its density by mercury displacement, 2.34 gm/cm^3.

Schwartz (7) also tested Indiana limestone in conventional triaxial tests. Table 1 outlines the variations between that rock and the CANMET specimens. Based on these variations it is doubtful that the two test programs used samples from the same geological horizon. This could partly account for the variation between the peak strength curves obtained then and now, Fig. 11.

Table 1 - Comparison of Indiana limestone tested

	Porosity (%)	Density $(gm/cm)^3$	Petrological description
Schwartz (7)	0.1935	2.19	"Light buff coloured oolitic limestone from the upper part of the stratum".
CANMET	0.1296+	2.34*	Buff coloured oolitic limestone with 30 to 50% fossils: pelecypods, gastropods, bryozoans.

+ measured by mercury porosimetry, 0.000784 cm^3/count.

* using mercury displacement.

EXPERIMENTAL SET-UP

A stiff triaxial assembly [the same one used by Shimotani (4)], Fig. 1-2, was used to obtain full triaxial response from rock specimens, pre- and

post-failure. The confinement to a Hoek pressure vessel was provided by a confining pressure panel capable of generating up to 205 MPa confining pressure [Gorski (6)]. A universal compression testing machine provided the vertical load through a hardened steel cylinder load cell. This cell was strain gauged to reproduce imparted micro-strains. Disc springs acted as a stiffening frame to reduce the total energy imparted to the sample by the compression machine. This and the operation of a magneto-electric valve which opens and shuts the hydraulic bypass of the testing machine for faster unloading than manual control unloading, permits the resolution of the rock behaviour in the post failure region.

This valve was developed by Mr. F. Kapeller of CANMET. Loading was applied at approximately 3×10^{-3} strain/min for all tests. LVDT's were used in conjunction with applied load to trace out the stress-strain curves and serving as a back-up for elastic modulus when the strain gauges were operational. The latter were used also to measure Poisson's ratio, and became a more sensitive indicator of failure onset compared to the LVDT's. On one X-Y-Y pen recorder, two curves were drawn; one with the load cell and LVDT signals yielding a stress-strain curve, one with the load cell and confining pressure signals. On another, the load versus sample deformation using strain gauges both axially and diametrically. Three strain indicators were used to visually monitor the axial, diametric and load cell strains during testing. An additional X-Time is used during the strain controlled testing to set the vertical loading rate at a suitable level for tracing the deformation modulus "p" as well as possible (too slow, and the sample becomes subject to too much microfracturing, too fast will make it very difficult to vary the confining pressure in time to prevent total sample failure).

THEORETICAL CONSIDERATIONS

MULTIPLE FAILURE STATE TEST

The advantage of this testing method lies in saving specimens and time to achieve the same results as a larger number of conventional triaxial tests.

Important considerations must be examined to explain the rock specimen behaviour during successive failure levels brought on by varying the confining pressure. The sample is never allowed to fail; the confining pressure

is increased just prior to attaining peak strength. The sample can thus sustain a return and increase or decrease in confining pressure, Fig. 3. Similarly, once residual strength is achieved various other residual levels can be reached, Fig. 4.

STRAIN-CONTROLLED TRIAXIAL TEST

The concept of this test is well illustrated by the alternate title "continuous failure state test", Kovari et al. (2). Beyond the peak strength obtained at a specific confining pressure, the specimen is forced into continuing failure state by increasing the confining pressure as well as vertical load. The stress-strain path followed, Fig. 5 describes a line with slope p, theoretically containing the peak strengths of the specimen at various confinement. The load is thus at peak for each confinement, Fig. 5. This slope is unique (within specimen variations) making the final failure level not dependent on the starting confining pressure.

The slope p to be followed can be determined a-priori from conventional or multistage tests (only one specimen test is necessary in this instance) with the obtained peak strengths (four at least of widely different confining pressures) (Fig. 5,8,9). Kovari et al. (2) have established an approximation to the slope p if it is not known a-priori; the general limits for the approximation may be set to:

$$0.5 \leq V/E \leq 1.0$$

where E is the modulus of elasticity, V the slope of the approximation.

It is evident from Fig. 5, (with E = V) that the overestimation of p defines an unfailed state after the first peak strength is passed; underestimation places the specimen under increased plastic strain and into the failed state, resulting with unrecoverable loss of strength. It is thus more preferable to overestimate p. Kovari et al. established these corrections for this case (see Fig. 5):

$$\Delta\sigma_{(\text{at } \sigma_{3_o} \leq \sigma_3 \leq \sigma_{3_n})} = \Delta\sigma_n \frac{\sigma_3 - \sigma_{3_o}}{\sigma_{3_n} - \sigma_{3_o}}$$

where

σ = axial stress

σ_3 = confining stress

o = original

n = final

In the case of lower p values the last maximum is never reached, thus, the peak strength line is not correctable.

RESULTS

MULTIPLE FAILURE STATE TEST

To validate this test, conventional triaxial tests were performed. Ten specimens were tested under several confining pressures, for both types of tests. Five confining pressure levels were used in the conventional tests, six for the multiple failure state tests, Table 2-3, Fig. 6,7.

The Mohr's stress envelopes for peak and residual strength are presented in Fig. 10. The measured values represent the envelope based on measured failure angles of tested specimens. The theoretical values Table 4, use functional relations between principal stresses advanced by Coates (8):

$$\frac{\sigma_1 + \sigma_c}{\sigma_3 + \sigma_c} = \tan^2 (45 + \phi/a) = f$$

$$\sigma_1 = \sigma_{3f} + \sigma_{cf} - \sigma_c$$

$$\sigma_1 = \sigma_{3f} + \sigma_c (f - 1)$$

where $\sigma_3 = 0$

$$\sigma_1 = \sigma_c (f - 1) = Qu$$

$$\therefore \sigma_1 = \sigma_{3f} + Qu$$

$$\underline{\text{or}} \quad \sigma_1 = \sigma_3 [\tan^2(45 + \phi/2)] + Qu$$

Table 2 - Conventional triaxial test results

σ_3	0 MPa						6.9 MPa				20.7 MPa				34.5 MPa				46.5 MPa			
	σ_1 peak (MPa)	ϵ_{peak} x 10^{-3}	E (GPa)	ν	$\sigma_{residual}$ (MPa)	L/D	σ_1 peak (MPa)	ϵ x 10^{-3}	$\sigma_{residual}$ (MPa)	L/D	σ_1 peak (MPa)	ϵ x 10^{-3}	$\sigma_{residual}$ (MPa)	L/D	σ_1 peak (MPa)	ϵ x 10^{-3}	$\sigma_{residual}$ (MPa)	L/D	σ_1 peak (MPa)	ϵ x 10^{-3}	$\sigma_{residual}$ (MPa)	L/D
	48.7	3.0	+/23.6*	-	-	2.00	89.2	4.6	51.8	2.04	124.5	6.0	111.0	1.99	146.3	8.7	143.5	2.00	168	17.1	168	2.00
	56.4	2.5	-/26.9	-	-	2.04	89.3	4.1	53.6	2.04	120.0	-	113.8	2.00	146.3	9.7	142.2	2.00				
	70.6	2.5	-/28.5	-	-	2.02	88.4	4.2	47.6	2.01	126.7	-	116.6	1.99	151.4	9.4	147.2	2.00				
	84.3	2.7	-/39.2	-	-	2.05	92.8	4.3	49.7	2.00	123.3	6.3	111.0	2.00	148.1	9.5	143.9	2.02				
	61.3	2.8	-/27.8	-	-	2.03	90.5	4.2	55.7	2.01	112.0	7.8	108.1	2.01	144.2	11.6	144.2	2.00				
	62.0	2.1	35.1/-	0.26	-	2.00	88.2	5.0	45.0	2.02	126.6	7.3	111.1	2.01	150.1	9.1	147.9	1.99				
	59.6	2.1	59.9/41.8	0.26	-	2.00	89.7	4.0	42.2	2.02	124.3	7.5	115.9	1.99	147.9	10.6	146.7	2.06				
	52.9	2.1	-/32.6	-	-	2.01	84.0	4.0	-	2.02	125.9	7.8	114.2	2.01	154.7	9.7	151.3	2.00				
	52.4	2.6	44.8/31.0	0.28	-	2.05	87.5	4.0	42.2	2.00	128.7	6.9	115.7	2.01	148.5	9.0	144.0	2.05				
	52.0	2.4	-/24.0	-	-	2.03	94.3	3.9	-	2.01												
	69.9	3.1	-/-	-	-	2.03																
	50.5	2.1	35.4/26.5	0.25	-	2.06																
Mean	59.7	2.5	43.8/29.8	0.26	-	2.03	89.3	4.2	48.5	2.02	123.6	7.1	113.0	2.00	148.6	9.7	145.7	2.01				
Standard Deviation	13.0	0.3	10.2/6.3	0.01	-	0.02	2.8	0.3	4.8	0.01	4.7	0.7	2.8	.01	3.1	0.8	2.7	0.02				

+ using strain gauges

* using LVDT's

- not available

Table 3 - Multiple failure state test results

σ_3	0 MPa						6.9 MPa			13.8 MPa			20.7 MPa			27.6 MPa			34.5 MPa		
	σ_1 peak (MPa)	ϵ_{peak} x 10^{-3}	E (GPa)	ν	$\sigma_{residual}$ (MPa)	L/D	σ_1 peak (MPa)	ϵ_p x 10^{-3}	$\sigma_{residual}$ (MPa)	σ_1 peak (MPa)	ϵ_p x 10^{-3}	$\sigma_{residual}$ (MPa)	σ_1 peak (MPa)	ϵ_p x 10^{-3}	$\sigma_{residual}$ (MPa)	σ_1 peak (MPa)	ϵ_p x 10^{-3}	$\sigma_{residual}$ (MPa)	σ_1 peak (MPa)	ϵ_p x 10^{-3}	$\sigma_{residual}$ (MPa)
	43.0	2.8	--/23.6*	-	4.6	2.01	83.0	4.5	61.7	102.8	5.9	92.8	119.5	7.0	115.5	134.4	8.7	134.0	147.2	11.4	146.0
	44.8	2.2	-/25.8	-	4.0	2.03	87.0	4.1	59.1	106.3	5.3	90.0	121.8	6.4	112.8	133.3	7.2	130.5	145.9	9.6	144.0
	52.5	2.3	33.1/30.9	0.26	7.5	2.00	86.3	4.0	62.9	106.2	5.2	93.3	121.3	6.7	116.2	135.8	8.2	135.1	148.1	11.4	147.0
	63.6	2.7	33.7/29.3	0.27	6.9	2.00	94.6	4.1	63.0	113.4	5.2	96.5	129.6	6.2	120.2	144.6	7.5	142.2	157.3	9.8	156.0
	59.2	2.7	35.7/29.0	0.27	6.5	2.09	92.2	4.3	64.0	112.1	5.6	94.9	128.8	7.0	119.0	143.9	8.4	140.2	157.2	10.2	154.7
	54.1	2.7	40.2/23.8	0.25	-	2.05	88.3	4.6	-	Pass	Pass	-	122.3	5.7	-	Pass	Pass	-	149.4	10.5	-
	43.3	2.4	34.3/22.9	0.24	-	2.06	83.6	4.5	-	Pass	Pass	-	123.7	7.2	-	Pass	Pass	-	149.6	11.1	-
	42.5	2.8	29.2/23.0	0.26	8.6	2.00	84.1	5.1	61.1	Pass	Pass	81.8	119.6	6.7	115.6	Pass	Pass	126.8	144.7	10.4	143.0
	45.6	2.1	59.5/26.7	0.22	8.6	2.03	79.7	4.6	60.6	Pass	Pass	88.1	113.2	7.6	108.6	Pass	Pass	127.2	140.8	11.6	140.8
	60.9	2.2	48.7/37.0	0.23	-	2.05	90.6	3.7	-	Pass	Pass	-	118.1	6.0	-	Pass	Pass	-	147.5	11.8	-
Mean	51.0	2.5	39.3/27.2	0.25	6.7	2.03	86.9	4.4	61.8	108.2	5.4	91.1	121.8	6.7	115.4	138.4	8.0	133.7	148.8	9.8	147.3
Standard Deviation	8.2	0.3	9.4/6.4	0.02	1.7	0.03	4.6	0.4	1.5	4.0	0.3	4.6	4.8	0.6	3.6	4.8	0.6	5.4	4.9	1.2	5.4

+ using strain gauges

* using LVDT's

- not available

Table 4 - Comparison of theoretical and measured failure properties for conventional and multiple failure state tests

σ_3 MPa	α_m^* Degrees	α_{th} Degrees	ϕ_m Degrees	ϕ_{th} Degrees	C_m MPa	C_{th} MPa
Conventional tests						
0	67.5	-	45.1	-	12.5	-
6.9	57.0	64.3	28.0	38.6	21	14.6
20.7	57.0	65.5	24.0	31.0	24.5	16.9
34.5	55.5	58.0	21.0	26.0	26.5	19.5
46.5	-	56.8	-	23.5	-	20.0
Multiple failure state tests						
0	-	-	-	-	-	-
6.9	-	66.3	-	42.6	-	11.6
13.8	-	63.8	-	37.7	-	12.5
20.7	-	61.6	-	33.2	-	13.5
27.6	-	60.7	-	31.4	-	14.2
34.5	55.5	59.3	21	28.5	26.5	14.5

Theoretical considerations, page 5

$\sigma_1 = \sigma_3 [\tan^2(45 + \frac{\phi}{2})] + Qu$

Qu = uniaxial compressive strength

* average

where σ_c = intrinsic stress resulting from intermolecular attraction
Qu = uniaxial compressive strength
α = 45 + ϕ/2 failure angle of specimen from horizontal axis
ϕ = internal angle of friction of the specimen.

Figures 11,12 depict the peaks and residual limit strength curves for the conventional multiple failure state tests, as well as the peak strength data of Schwartz (7) and Mogi's (10) brittle-ductile transition criterion.

The residual strength data of the multiple failure state tests was obtained once the last stage's residual was reached, by decreasing the confining pressure while maintaining axial rock deformation.

Table 2,3 present respectively the conventional and multiple failure state test results.

The uniaxial properties of Indiana limestone, using conventional testing are: peak strength 59.7 ± 13.0 MPa, accompanied by a strain (x 10^{-3}) of 2.5 ± 0.3, the modulus of elasticity, using LVDT's, is 29.8 ± 6.0 GPa and Poisson's ratio is 0.26 ± 0.1. For the 6.9 MPa, 20.7 MPa and 34.5 MPa confining pressures the peak strength, related strain (x 10^{-3}) and residual strength respectively are: 89.3 ± 2.8 MPa, 4.2 ± 0.3, 48.5 ± 4.8 MPa; 123.6 ± 4.7 MPa, 7.1 ± 0.7, 113.0 ± 2.8 MPa; 148.6 ± 3.1 MPa, 9.7 ± 0.8, 145.7 ± 2.7 MPa. The brittle-ductile transition occurred at 168 MPa load, 46.5 MPa confinement, strain of 17.1 x 10^{-3}.

The uniaxial properties of Indiana limestone, using multiple failure state tests are: peak strength 51.0 ± 8.2, MPa accompanied by a strain (x 10^{-3}) of 2.5 ± 0.3, a residual strength of 6.7 ± 1.7 MPa; the modulus of elasticity is 27.2 ± 6.4 GPa and Poisson's ratio is 0.25 ± 0.02. For the 6.9 MPa, 13.8 MPa, 20.7 MPa, 27.6 MPa and 34.5 MPa confining pressures, the peak strength, related strain (x 10^{-3}) and residual strength repspectively are: 86.9 ± 4.6 MPa, 4.4 ± 0.4, 61.8 ± 1.5 MPa; 108.2 ± 4.0 MPa, 5.4 ± 0.3, 91.1 ± 4.6 MPa; 121.8 ± 4.8 MPa, 6.7 ± 0.6, 115.4 ± 3.6 MPa; 138.4 ± 4.8 MPa, 8.0 ± 0.6, 133.7 ± 5.4 MPa; 148.8 ± 4.9 MPa, 9.8 ± 1.2, 147.3 ± 5.4 MPa.

Observing that the elastic modulus, using gauges, is very high compared with that obtained using LVDT's, and that the standard deviation from the mean is also high, it is suspected that the limestone porosity has affected the bonding ability of the gauge adhesive, precluding accurate transmission of strain behaviour. The LVDT results are thus adopted, and the value of Poisson's ratio questioned.

On previous occasions, with rock types that permitted proper gauge function, the authors experienced lower modulus of elasticity values for LVDT's with respect to gauge values, by a factor of approximately 10%. It is possible then that more representative values for the Indiana limestone modulus be higher.

STRAIN CONTROLLED TEST

The slope p obtained from conventional and multiple failure state results (Fig. 8,9) is not constant, decreasing from 18 (at σ_3 = 6.9 MPa) to approximately 6 GPa, (at σ_3 = 34.5 MPa). The value used in each strain control test, because it is constant, will not produce the true limit strength curve. From the five slopes adopted for the strain control tests (p = 15 GPa, 17.5 GPa, 19 GPa, 23.5 GPa, 27.5 GPa) Fig. 13-17, it is shown that the value of p at σ_3 = 6.9 is indeed approximately 18 GPa, and decreases rapidly with increasing confining pressure (Fig. 14 - increasing departure of strain control "limit strength curve" from that established by the other triaxial tests).

TEST RESULTS

At all confining pressures greater than zero, the conventional triaxial tests yield information identifying Indiana limestone as a Class I rock type [Wawersik (3)]. Its immediate post peak behaviour indicates that energy is required to advance the failure of the sample; at zero confinement the behaviour is transitional between Class I and II.

Based on averages, the results of the multiple failure state tests compare very favourably with the corresponding conventional test results. Both peak strength and the strain at that level follow this comparison, at all, except 6.9 MPa, confining pressures. The standard deviations for corresponding results are also very similar. The small difference in peak strength values between the two tests is expected, since the sample during a multiple failure state test is elevated to a higher confining pressure just before what seems to be the onset of peak strength. As well, the specimen carries forward the strain and microfracturing induced in the first stage of the multiple failure state test.

In the strain controlled tests the amount of departure from the average limit strength curve does increase with higher overestimation, as

predicted by Kovari et al (2). This is shown, as mentioned earlier, within one strain-controlled test. The p value decreases with increasing confining pressure. Thus each test that begins with an overestimation of p (i.e., p>~18 GPa) will remain in overestimation, displaying increasing departures from the true limit strength curve as the test advances to higher confining pressure. The Kovari et al. correction, Table 5, for overestimated p values in our case falls short of the actual measured departures from the average limit strength curve no doubt because p decreases and that this prediction is based on a constant p. Testing of a number of other specimens may explain this discrepancy.

Table 5 - Prediction of departure from limit strength curve for p = E = 27.5 GPa

Confining pressure σ_3	0 MPa	6.9 MPa	13.8 MPa	20.7 MPa	27.6 MPa	34.5 MPa
Measured departure $\Delta\sigma$ (MPa) (Fig. 16)	-	0	30.3	32.0	32.0	36
Predicted departure $\Delta\sigma$ (MPa) (using *)	-	0	9.0	18.0	27.0	36

$$\sigma_{3_o} = 6.9 \text{ MPa}$$

measured $\Delta\sigma_n = 36$ MPa

$$\Delta\sigma^*(\text{at } \sigma_{3_o} \leq \sigma_3 \leq \sigma_{3_n}) = \Delta\sigma_n \frac{\sigma_3 - \sigma_{3_o}}{\sigma_{3_n} - \sigma_{3_o}}$$

COMPARISON OF INDIANA LIMESTONE TYPES

The difference from Schwartz's (8) results Fig. 11, can be attributed to a higher porosity, lower density type of Indiana limestone. The size dif-

ference, 2.2 cm diameter (3.8 cm length) compared to 4.2 cm diameter (8.2 cm length) for the CANMET samples, should theoretically result in a higher limit strength curve.

SPECIMEN BEHAVIOUR

Theoretical and measured comparisons of failure surface angle α, Table 4, indicate less disparity with measuring normal load. This tends to follow Terzaghi's (9) observation that, as pure shear failure is approached the slope angle of the failure surface can be successfully predicted by the Mohr envelope. Visual evaluation of specimen failure surfaces indicate tensile (intergranular parting) failure at uniaxial stress and predominantly shear (intragranular breaking) at confining pressures of 34.5 MPa.

HOEK AND BROWN FAILURE CRITERIA

Another evaluation of data that can be applied is the Hoek and Brown (5) empirical failure criterion for intact and broken rock, Appendix 1-4.

$$\sigma_1 = \sigma_3 + \sqrt{m\ \sigma_c\ \sigma_3 + s\ \sigma_c^2}$$

in which:

m, s are constants which depend upon the properties of the rocks, and upon the extent to which it has been broken before being subjected to σ_1, σ_3.

s = 1 for intact rock; σ_c is the uniaxial compressive strength, of intact rock material in the specimen.

As reported by Hoek and Brown it yields m = 3.2 for intact Indiana limestone tested by Schwartz.

The CANMET values for m, intact rock, are 3.7 and 5.2 for the conventional and multiple failure state tests, respectively. The departure from the Schwartz results originates from the higher values of deviator stress, Fig. 11;
deviator stress directly influences the regression calculations of m and s, Appendix 1-4.

The m and s values for broken Indiana limestone (at residual strength) are 5.3, 0.06 for conventional tests and 6.4, 0.14 for multiple failure state tests. The s values for the broken rock are lower than unity, intact rock, at a level indicating a high breakdown of cohesion and intergranular bonding, residual strength. Hoek and Brown (5) present such an unusual example where m is higher for broken rock, a granulated marble specimen. The failure surface(s) established after failure restricts intergranular bonding to asperity shearing. The increase in m for CANMET residual strength could hinge on the value of σ_c used. Calculating m requires an intact rock σ_c. During residual, the basic unit of interlocking aggregate becomes a grain, expected to have a higher value of σ_c than intact rock. The moderately cemented mass of fossils would tend to be granulated along the failure planes, after failure.

Finally, the reason for lower values, m and s, of the conventional tests compared to the multiple failure tests lies within the variation of input data and its effect on the regression calculations.

BRITTLE-DUCTILE TRANSITION

The Mogi (10) brittle-ductile transition criteria is:

$$\sigma_1 = 3.4\ \sigma_3$$

whereas the Indiana limestone tested at MRL is:

$$\sigma_1 = 3.7\ \sigma_3$$

CONCLUSIONS

- At all confinement greater than zero the post-peak behaviour of Indiana limestone is a reflection of a Class II rock type a "less brittle" rock type; at zero confinement it is transitional between I and II.

- Both peak strength and strains are very similar for the conventional and multiple failure state tests. The validity of the latter is thus assured.

- The results of the strain control test show that the limit strength curve can be obtained by either using a-priori conventional or multiple failure

state results, or setting the deformation slope p equal to the modulus of elasticity and correcting the limit strength curve results.

- The deformation slope p for Indiana limestone decreases considerably from 0 to 34.5 MPa confining pressure.

- The changing deformation slope p renders corrections to the limit strength curve difficult to formulate.

- The brittle-ductile transition for Indiana limestone occurs at low confining pressure: peak strength at 168 MPa and confining pressure of 46.5 MPa.

- Departures between theoretical and measured Mohr failure envelopes decrease with increasing load where the specimen becomes more subject to shear rather than to tensile failure.

- Hoek and Brown's (5) empirical relationship for failure of intact and discontinuous rock is representative of the results obtained for multiple failure state or conventional triaxial tests performed on Indiana limestone.

ACKNOWLEDGEMENTS

The authors are indebted to the following persons: Mr. M. Gyenge for his helpful advice on theoretical points and testing procedures; Mr. B. Gorski for providing practical services during the experimentation phase and to the students P. Friedrich and M. Balthazar for their consciencious cooperation during preparation and testing.

REFERENCES

1. Kovari, K. and Tesa, A. "Multiple failure state and strain controlled triaxial tests"; Rock Mechanics, 7, p 17-33; 1975.

2. Kovari, K., Tesa, A. and Attinger, R.O. "The concept of 'Continuous Failure State' triaxial tests"; Rock Mechanics, 16, p 117-131; 1983.

3. Wawersick, W.R. and Brace, W.F. "Post failure behaviour of an arenite and diabase"; Rock Mechanics, 3, p 81-85; 1971.

4. Shimotani, T. "Evaluation of testing procedures for minimizing rock sample requirement"; Division Report MRP/MRL 83-19(INT); CANMET, Energy, Mines and Resources, Canada; 1983.

5. Hoek, E. and Brown, E.T. "Underground excavations in rock"; Institution of Mining and Metallurgy, 527 pp; 1980.

6. Gorski, B. "The design and operation of a stiff triaxial assembly for post failure rock property testing"; Division Report MRP/MRL 82-81(TR); CANMET, Energy, Mines and Resources, Canada; 1982.

7. Schwartz, A.E. "Failure of rock in the triaxial shear test"; Proceedings of the Sixth Symposium on Rock Mechanics, University of Missouri at Rolla, p 109-135; 1964.

8. Coates, D.F. "Rock mechanics principles"; Monograph 874; Energy, Mines and Resources, Canada; 1981.

9. Terzaghi, K. "Stress conditions for the failure of saturated concrete and rock"; American Society for Testing Materials Proceedings, 45, p 777-801; 1945.

10. Mogi, K. "Pressure dependence of rock strength and transition from brittle fracture to ductile flow"; Bulletin of the Earthquake Research Institute, 44, p 215-232; 1966.

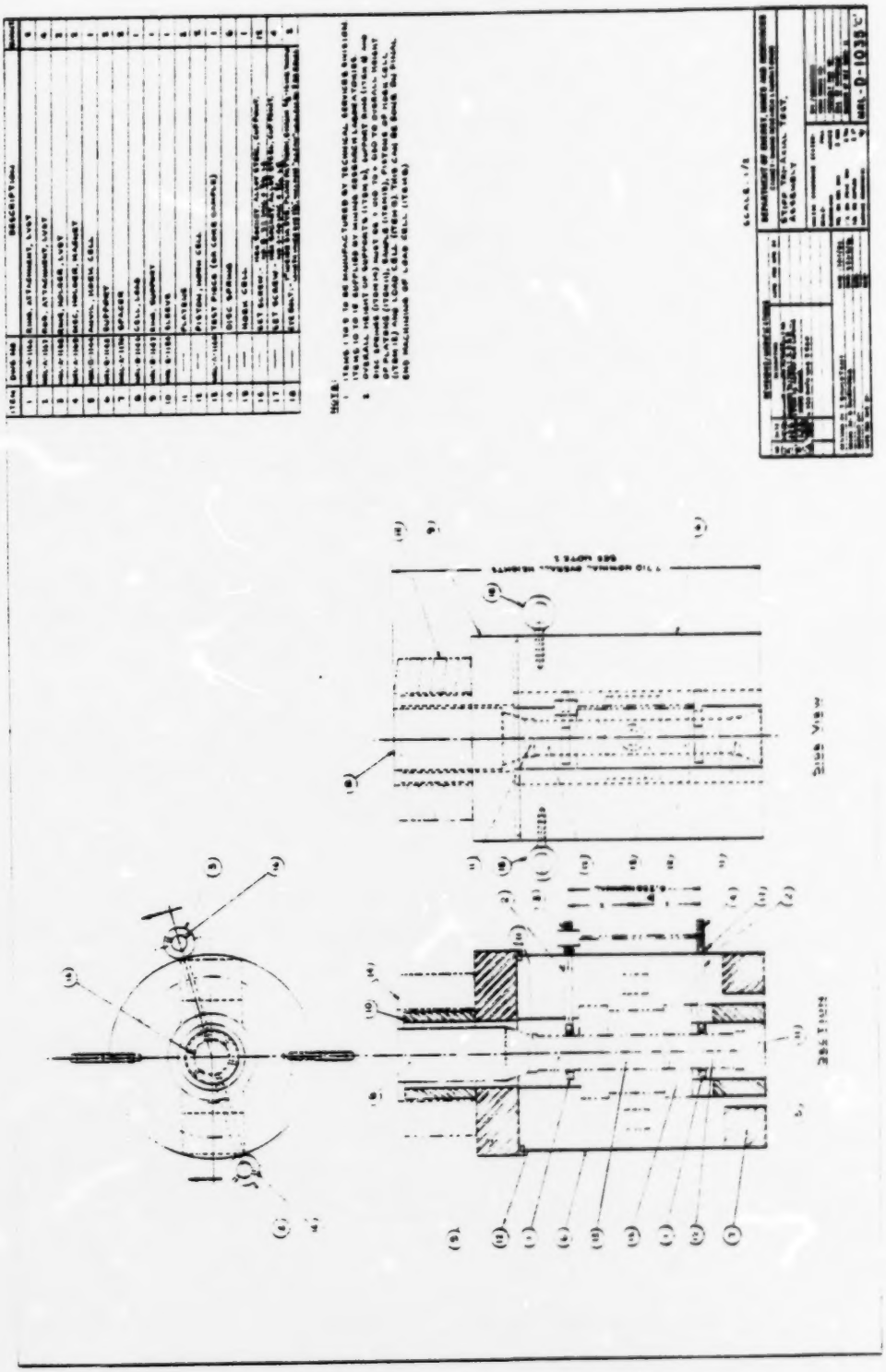

Fig. 1 - Triaxial stiff testing assembly.

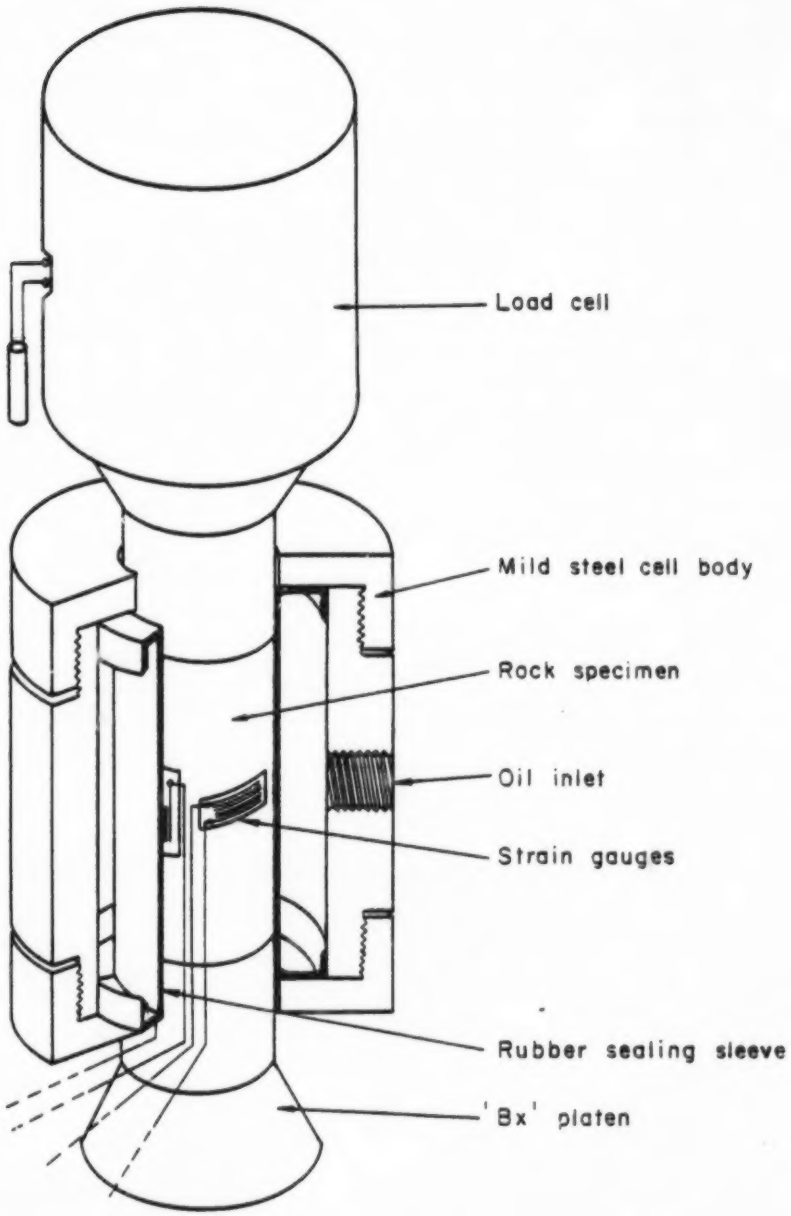

Fig. 2 - Details of the Hoek triaxial pressure vessel.

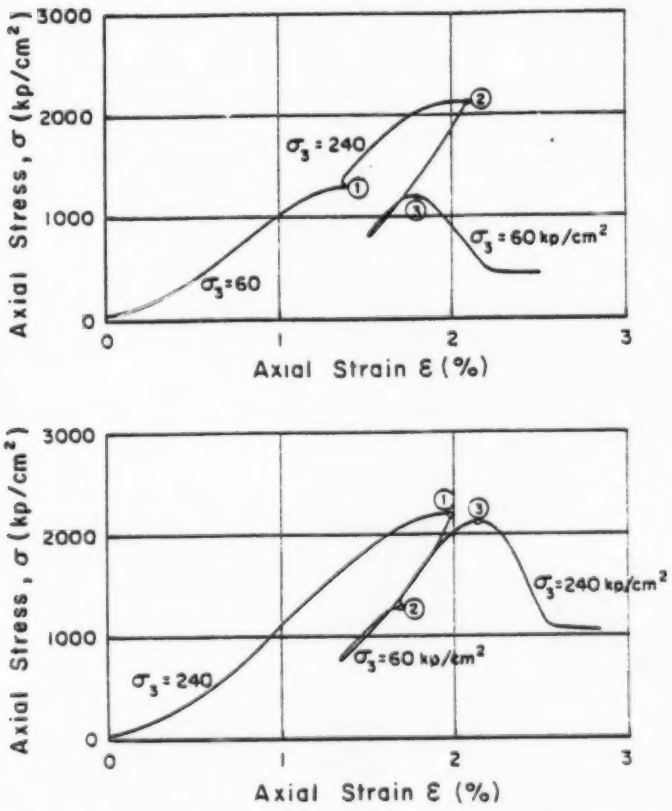

Fig. 3 - Sample behaviour at peak compressive strength with varying confining pressure (after Kovari and Tisa, 1975).

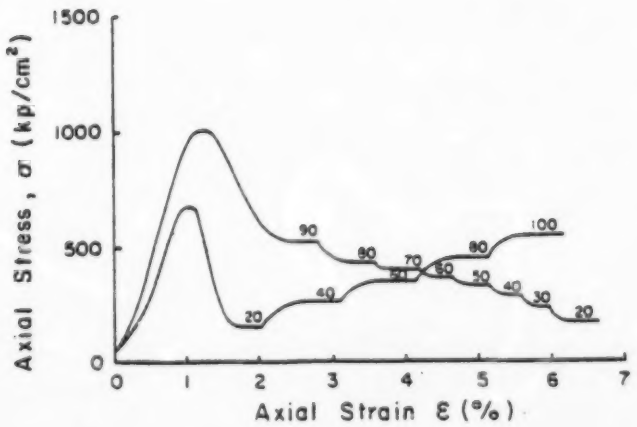

Fig. 4 - Sample behaviour at residual compressive strength with varying confining pressure (after Kovari and Tisa, 1975).

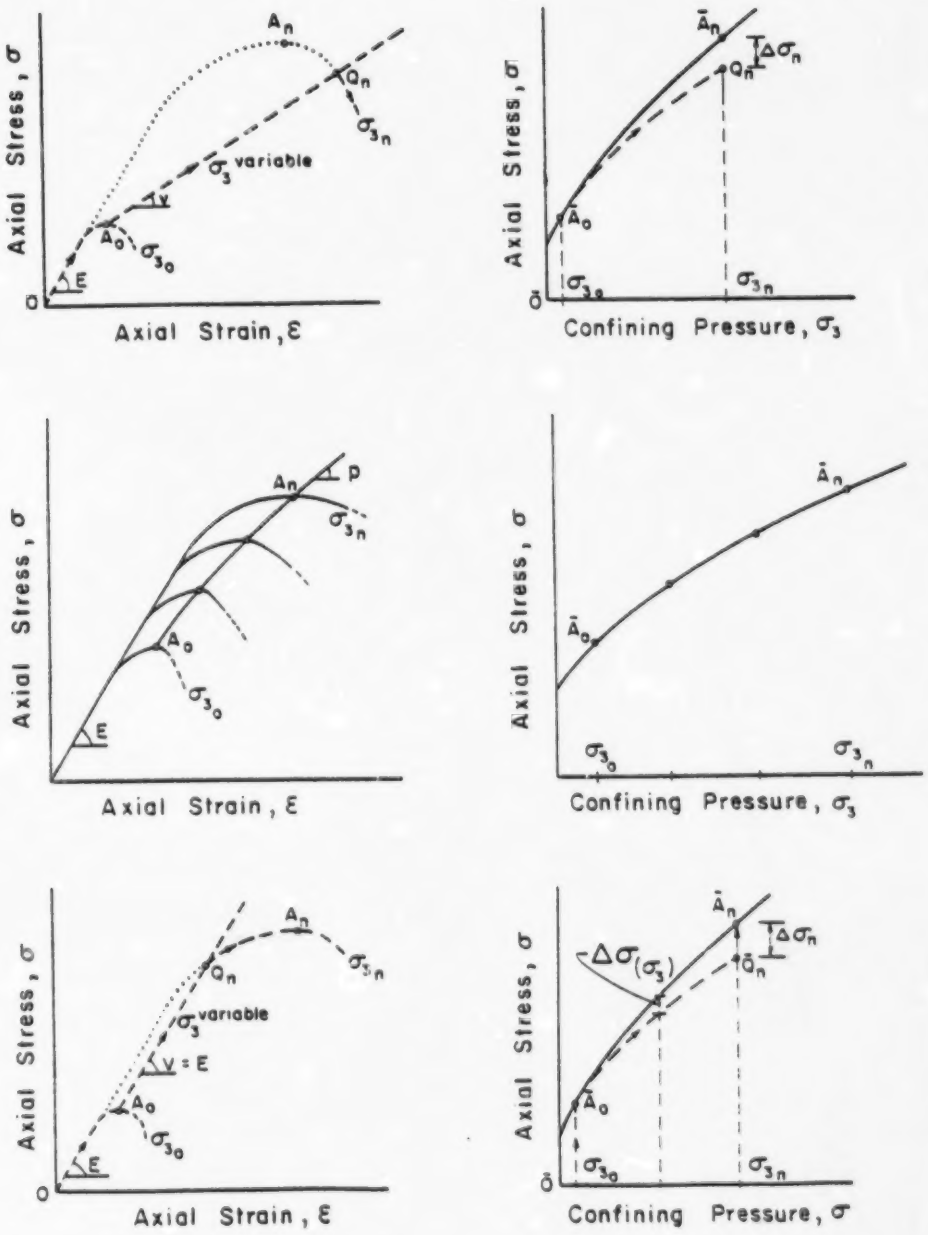

Fig. 5 - Strain controlled triaxial compressive tests with overestimation, proper estimation and under estimation of slope p. (After Kovari et al 1983).

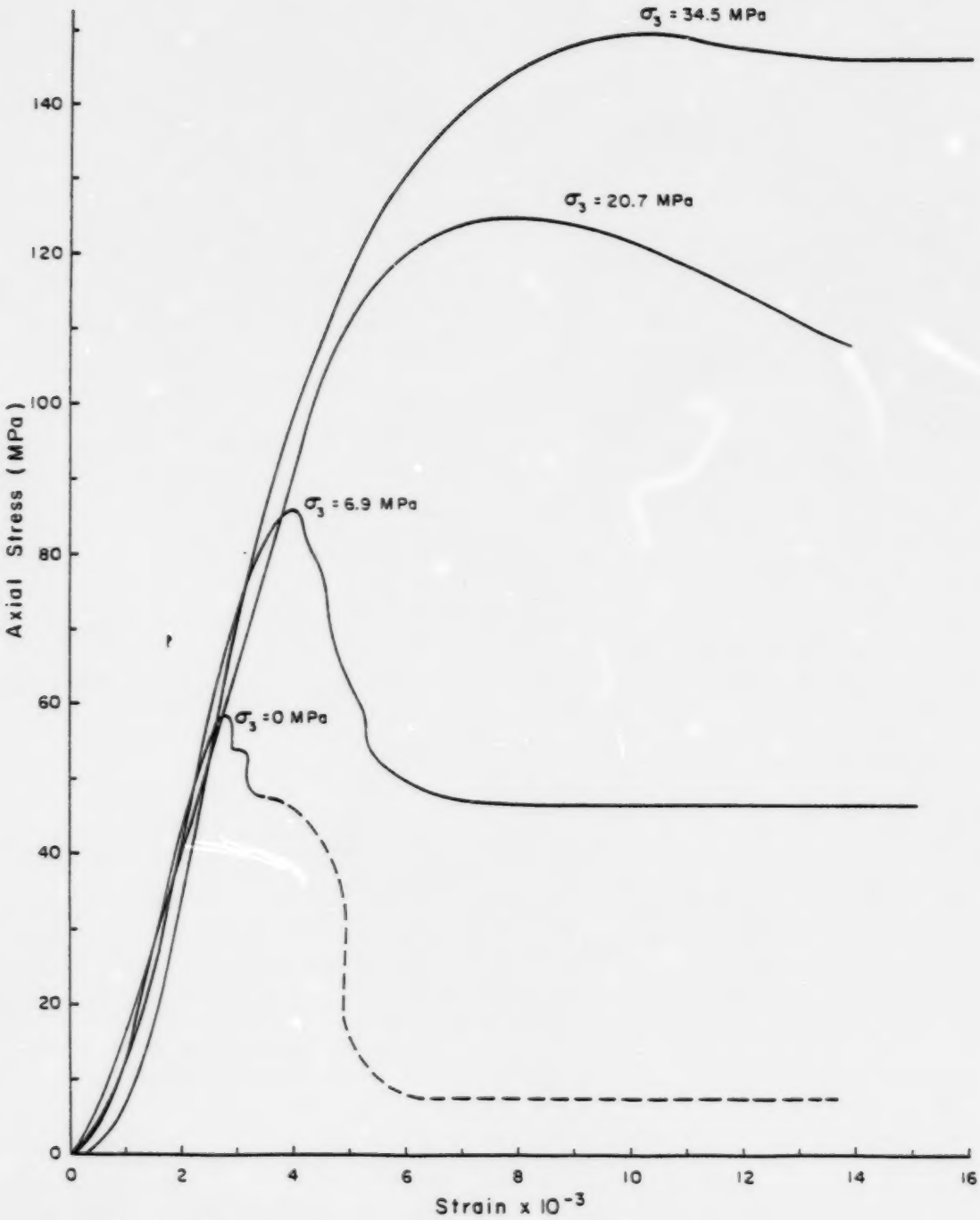

Fig. 6 - Conventional triaxial compressive test results of Indiana Limestone (using averages).

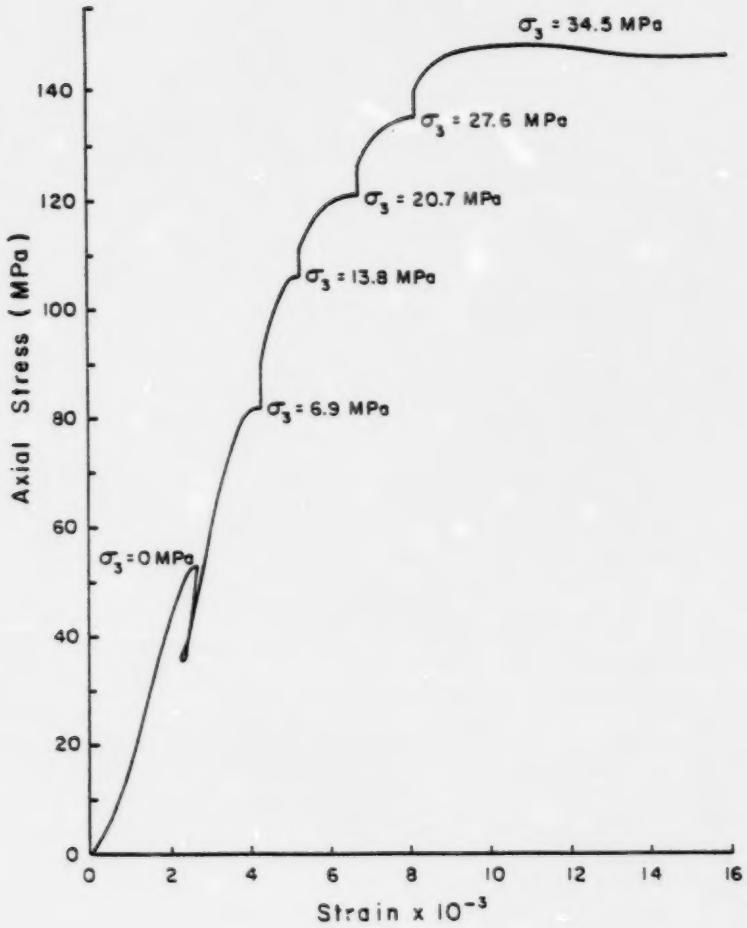

Fig. 7 - Multiple failure state compressive test results of Indiana Limestone (using averages).

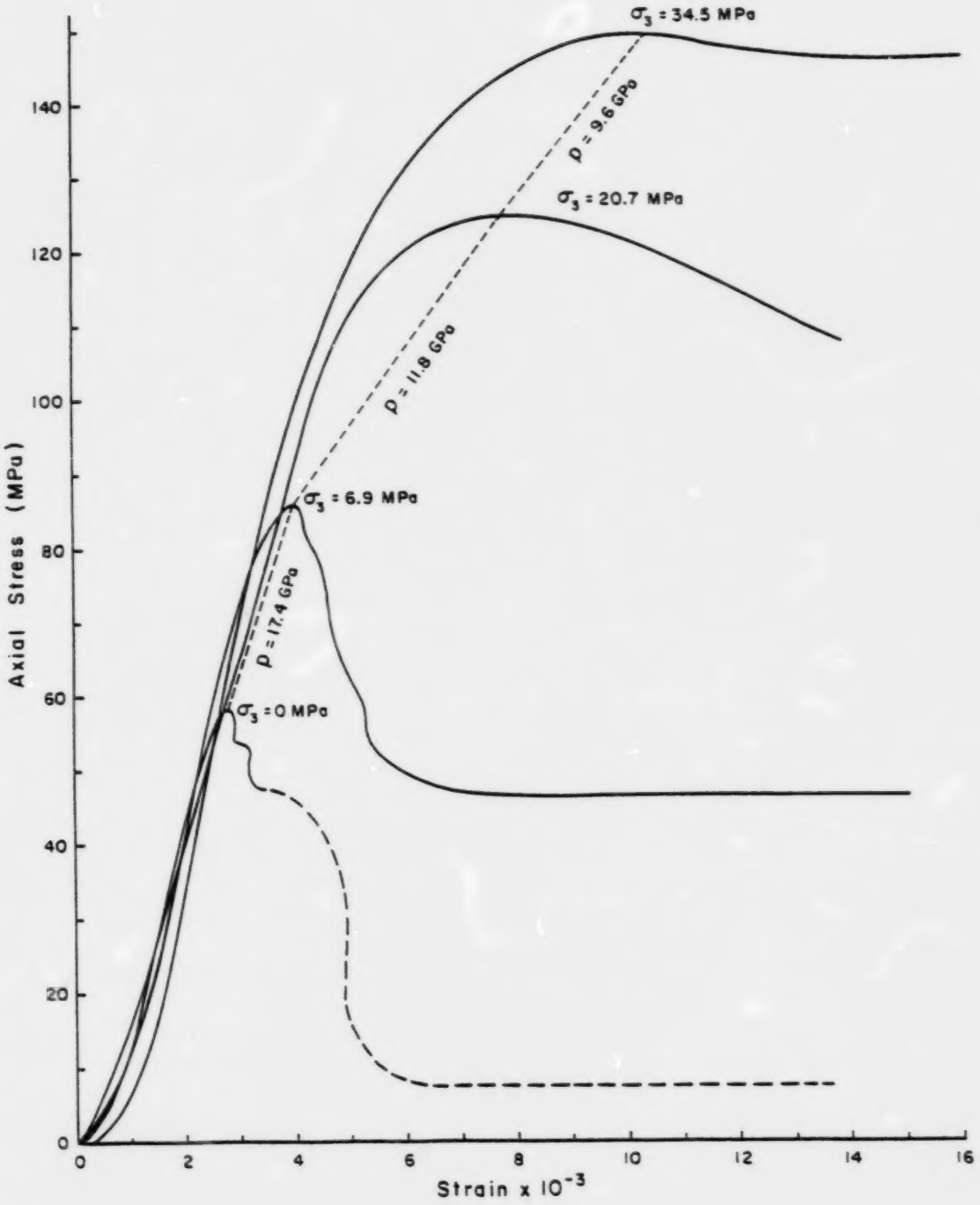

Fig. 8 - Stress-strain slope p of peak compressive strengths, conventional triaxial tests (using averages).

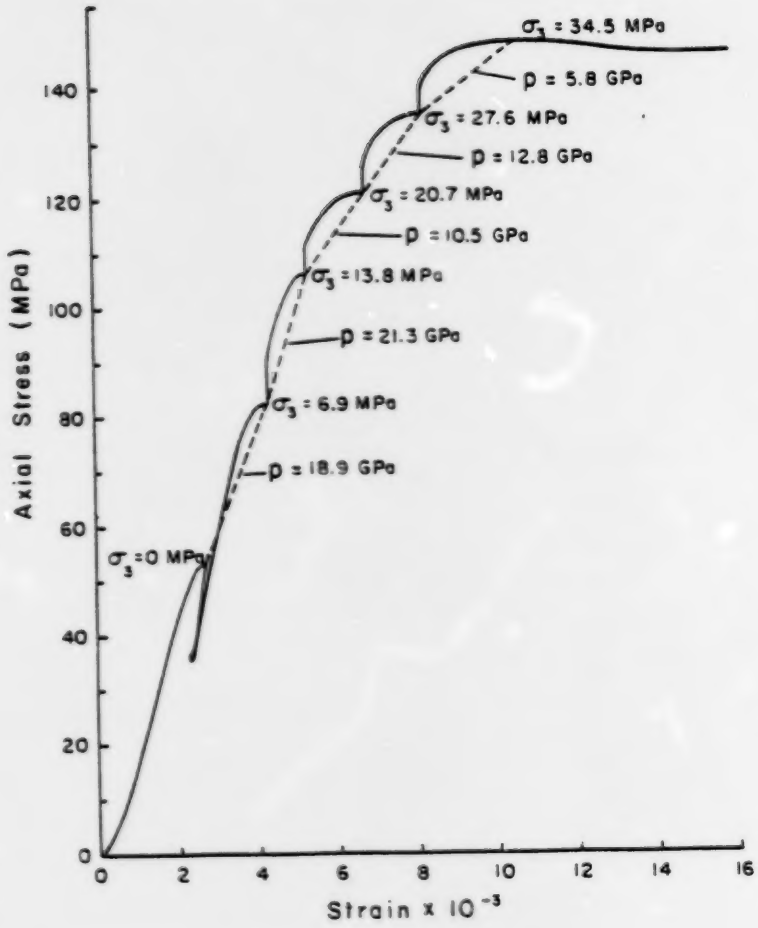

Fig. 9 - Stress-strain slope p of peak compressive strengths, multiple failure state test (using averages).

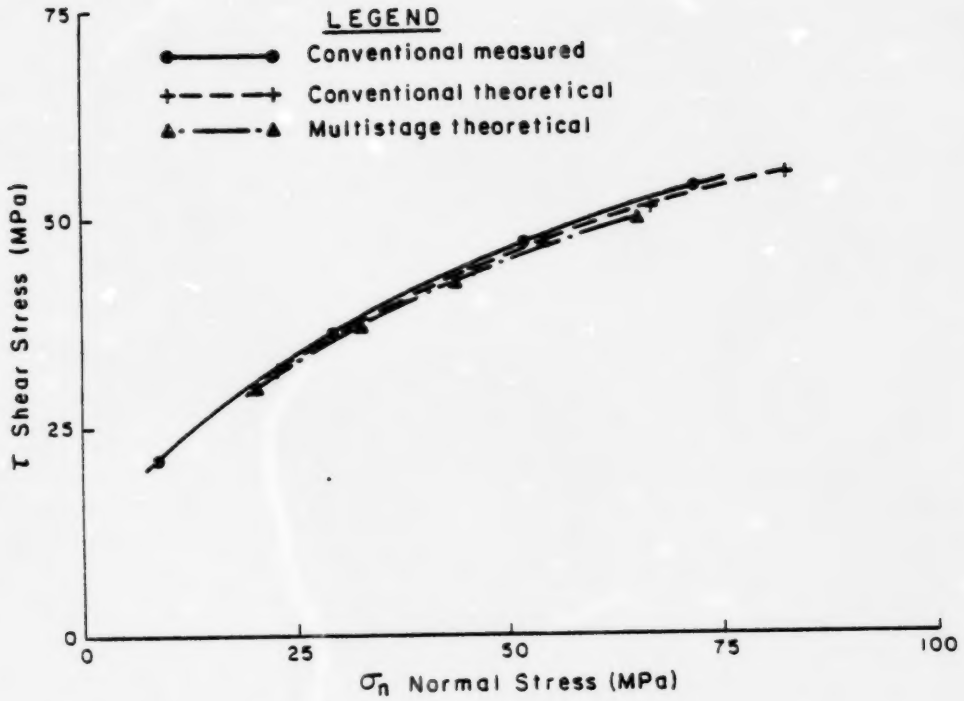

Fig. 10 - Mohr's peak stress envelope for theoretical and measured failure planes.

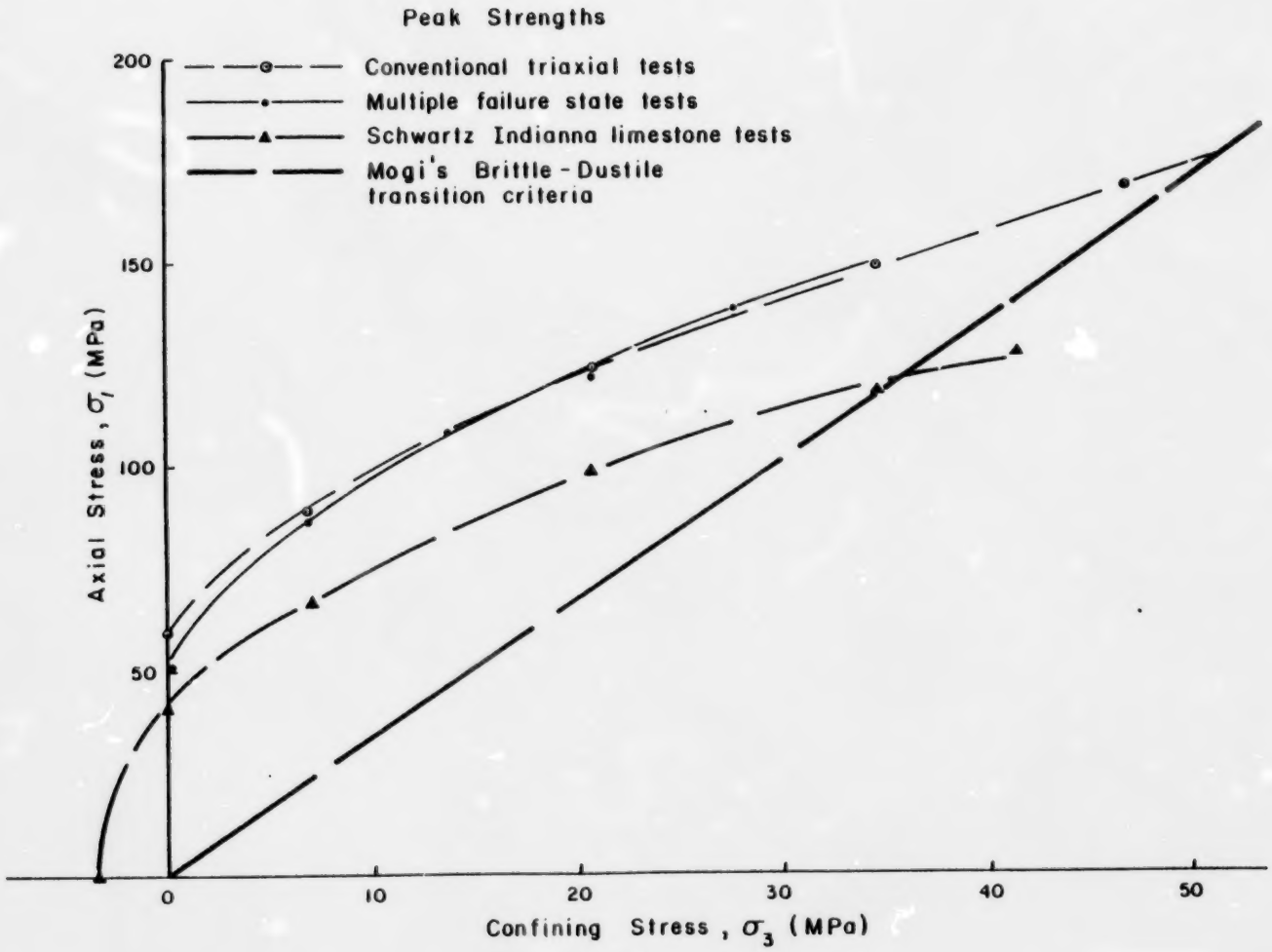

Fig. 11 - Limit strength curve for peak strength, conventional and multiple failure state compressive tests.

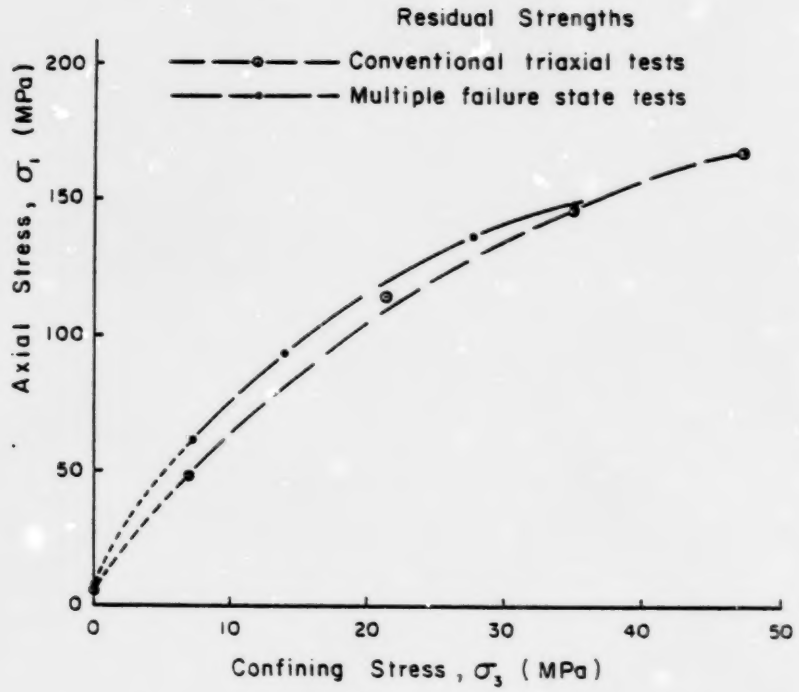

Fig. 12 - Limit strength curve for residual strength, conventional and multiple failure state compressive tests.

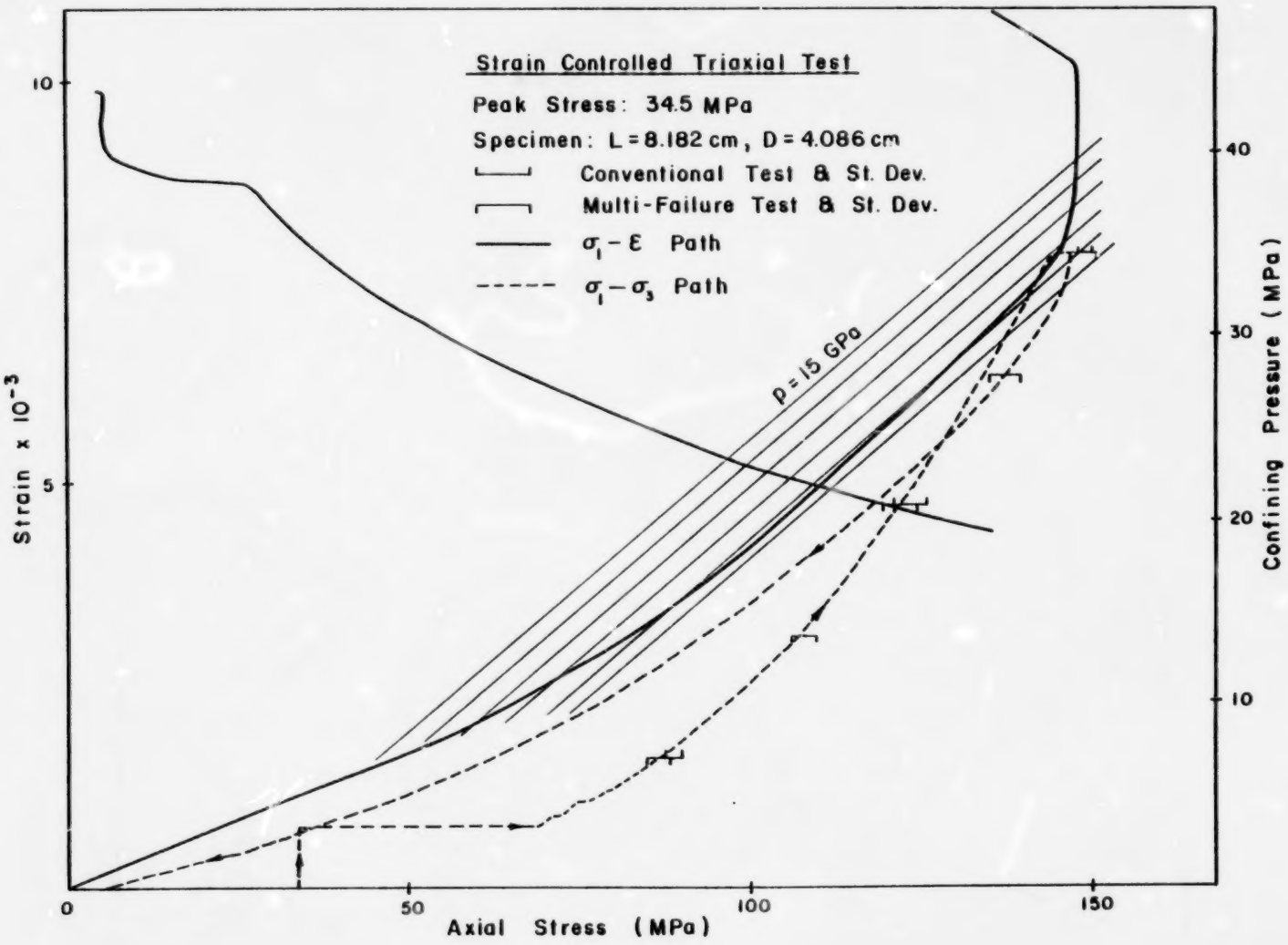

Fig. 13 - Strain controlled triaxial compressive test result, p = 15 GPa.

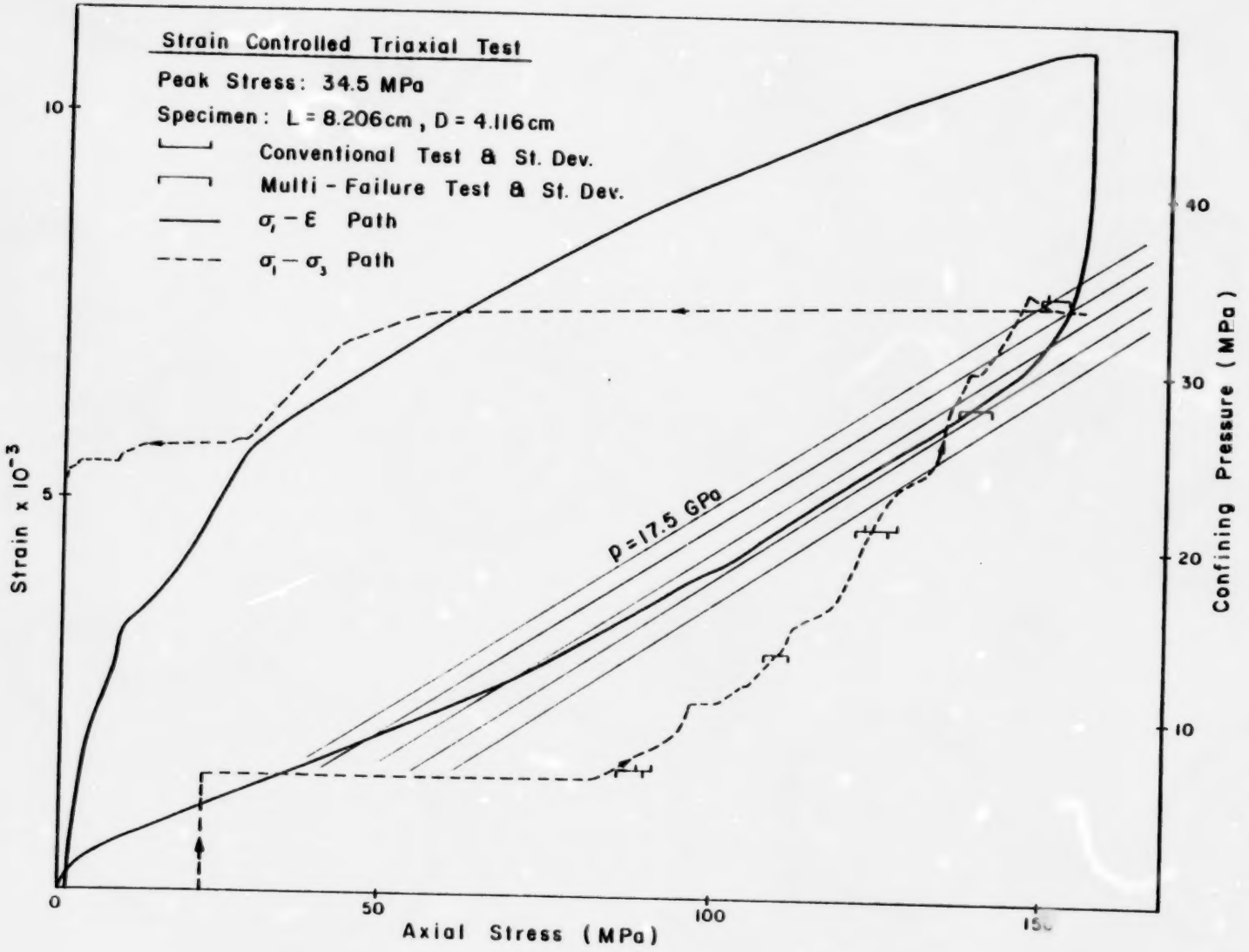

Fig. 14 - Strain controlled triaxial compressive test result, p = 17.5 GPa.

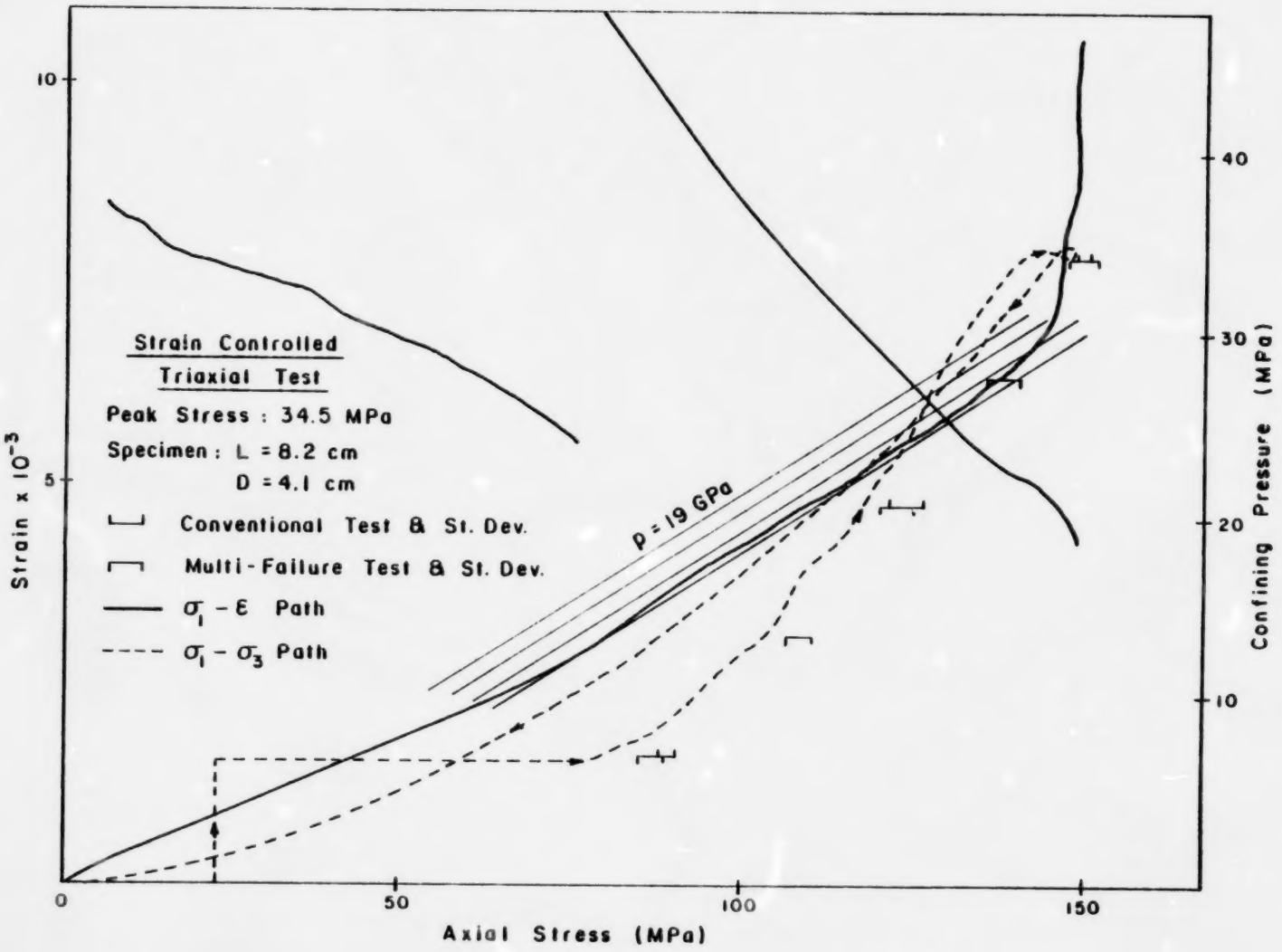

Fig. 15 - Strain controlled triaxial compressive test result, p = 19 GPa.

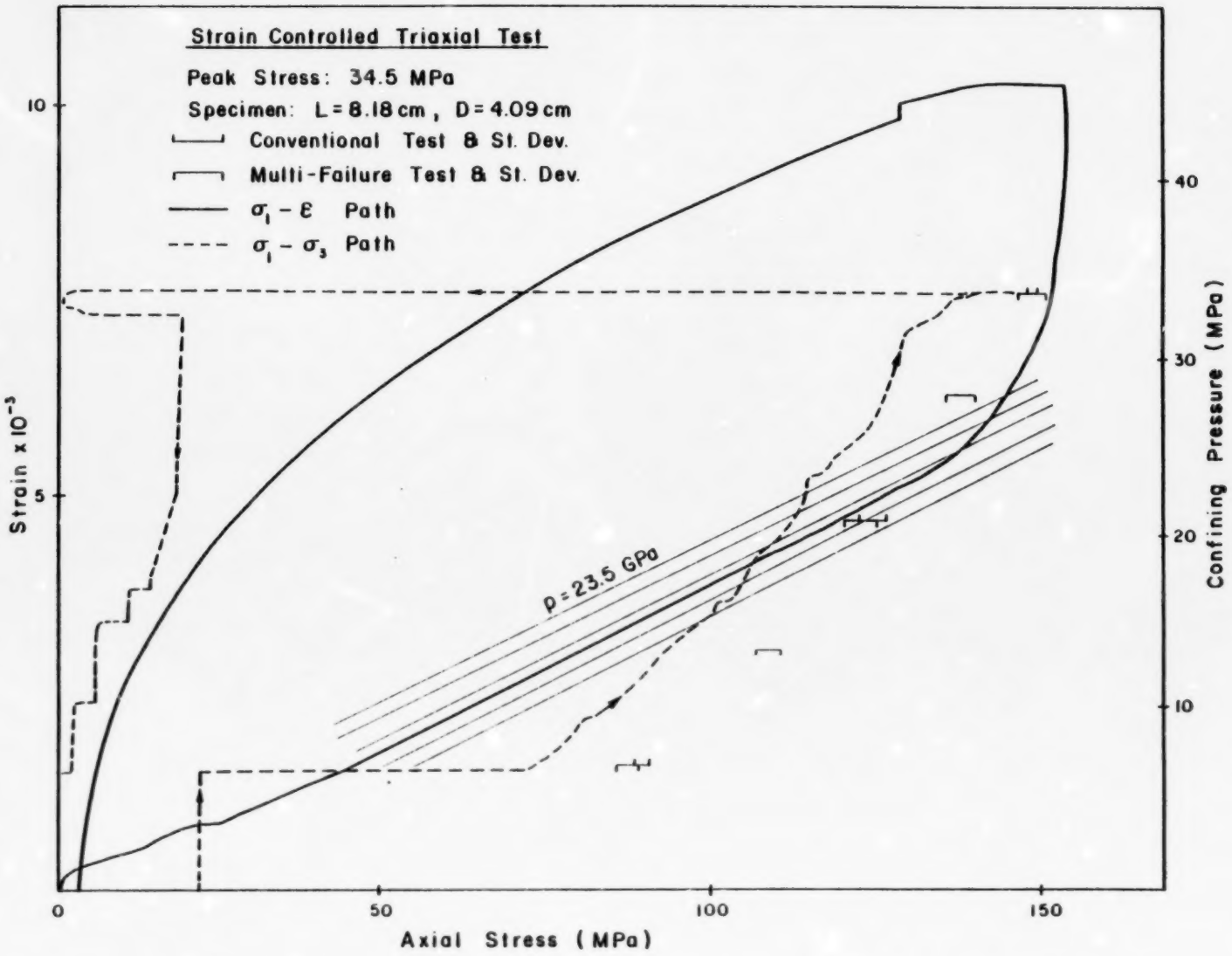

Fig. 16 - Strain controlled triaxial compressive test result, p = 23 GPa.

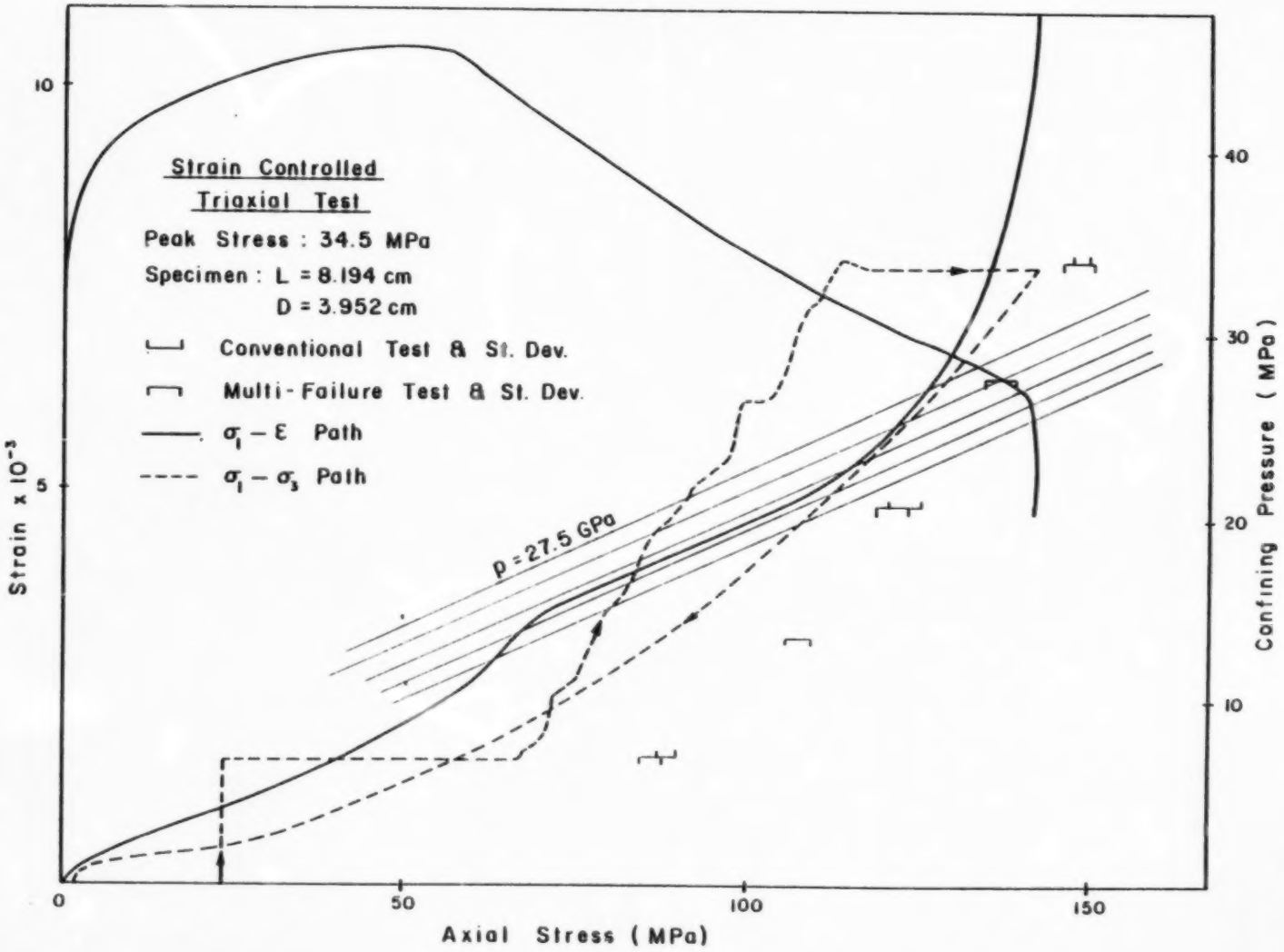

Fig. 17 - Strain controlled triaxial compressive test result, p = 27.5 GPa.

APPENDIX 1

DETERMINATION OF MATERIAL CONSTANTS FOR HOEK AND BROWN'S EMPIRICAL EQUATION, USING CONVENTIONAL TEST RESULTS

$$\sigma_1 = \sigma_3 + \sqrt{m\,\sigma_c\,\sigma_3 + s\,\sigma_c^2}$$

FOR INTACT ROCK

	x_i	y_i	$x_i y_i$	x_i^2	y_i^2
	0	3564	0	0	13351716
	6.9	6790	46581	48	46104100
	20.7	10588	219172	429	112105744
	34.5	13018	4491219	1190	169468324
	46.5	14762	686445	2162	217916644
Σ	108.6	48722	1401589	3828	558946528
Σ^2	11794	2373842054			

$y = (\sigma_1 - \sigma_3)^2 \quad x = \sigma_3 \quad s = 1 \quad n = 5$

$$\sigma_c^2 = \frac{\Sigma y_i}{n} - \left[\frac{\Sigma x_i y_i - \frac{\Sigma x_i \Sigma y_i}{n}}{\Sigma x_i^2 - \frac{(\Sigma x_i)^2}{n}} \right] \frac{\Sigma x_i}{n}$$

$$m = \frac{1}{\sigma_c} \left[\frac{\Sigma x_i y_i - \frac{\Sigma x_i \Sigma y_i}{n}}{\Sigma x_i^2 - \frac{(\Sigma x_i)^2}{n}} \right]$$

$$r^2 = \frac{\left[\Sigma x_i y_i - \frac{\Sigma x_i \Sigma y_i}{n} \right]^2}{\left[\Sigma x_i^2 - \frac{(\Sigma x_i)^2}{n} \right] \left[\Sigma y_i^2 - \frac{(\Sigma y_i)^2}{n} \right]}$$

$\sigma_c = 62.9$ MPa

$m = 3.7$

$r^2 = 0.95$

APPENDIX 2

DETERMINATION OF MATERIAL CONSTANTS FOR HOEK AND BROWN'S EMPIRICAL EQUATION, USING CONVENTIONAL TEST RESULTS

$$\sigma_1 = \sigma_3 + \sqrt{m\,\sigma_c \cdot \sigma_3 + s\,\sigma_c^2}$$

FOR BROKEN ROCK

	x_i	y_i	$x_i y_i$	x_i^2	y_i^2
	0	45	0	0	2025
	6.9	1730	11937	48	2992900
	20.7	8519	176343	429	72573361
	34.5	12354	426213	1190	152621316
	46.5	14762	686433	2162	217916644
Σ	108.6	37410	1300926	3829	446106246
Σ^2	11794	1399508100			

$y = (\sigma_R - \sigma_3)^2 \qquad x = \sigma_3 \qquad n = 5$

σ_c to be used = intact rock = 62.9 MPa

$$m = \frac{1}{\sigma_c}\left[\frac{\Sigma x_i y_i - \frac{\Sigma x_i \Sigma y_i}{n}}{\Sigma x_i^2 - \frac{(\Sigma x_i)^2}{n}}\right]$$

$$s = \frac{1}{\sigma_c^2}\left[\frac{\Sigma y_i}{n} - m\,\sigma_c \frac{\Sigma x_i}{n}\right]^2$$

$$r^2 = \frac{\left[\Sigma x_i v_i - \frac{\Sigma x_i \Sigma v_i}{n}\right]^2}{\left[\Sigma x_i^2 - \frac{(\Sigma x_i)^2}{n}\right]\left[\Sigma v_i^2 - \frac{(\Sigma v_i)^2}{n}\right]}$$

$m = 5.3$

$r^2 = 0.98$

$s = 0.06$

APPENDIX 3

DETERMINATION OF MATERIAL CONSTANTS FOR HOEK AND BROWN'S EMPIRICAL EQUATION, USING MULTIPLE FAILURE STATE TEST RESULTS

$$\sigma_1 = \sigma_3 + \sqrt{m\,\sigma_c\,\sigma_3 + s\,\sigma_c^2}$$

FOR INTACT ROCK

	x_i	y_i	$x_i y_i$	x_i^2	y_i^2
	0	1945	0	0	3783025
	6.9	6400	44160	48	40960000
	13.8	8911	122972	190	79405921
	20.7	10221	211575	429	104468841
	27.6	12276	338817	762	150700176
	34.5	13064	450708	1190	170668096
Σ	103.5	52817	1168232	2619	549986059
Σ^2	10712	2789635489			

$y = (\sigma_1 - \sigma_3)^2 \quad x = \sigma_3 \quad s = 1 \quad n = 6$

$$\sigma_c^2 = \frac{\Sigma y_i}{n} - \left[\frac{\Sigma x_i y_i - \frac{\Sigma x_i \Sigma y_i}{n}}{\Sigma x_i^2 - \frac{(\Sigma x_i)^2}{n}}\right]\frac{\Sigma x_i}{n}$$

$$m = \frac{1}{\sigma_c}\left[\frac{\Sigma x_i y_i - \frac{\Sigma x_i \Sigma y_i}{n}}{\Sigma x_i^2 - \frac{(\Sigma x_i)^2}{n}}\right]$$

$$r^2 = \frac{\left[\Sigma x_i y_i - \frac{\Sigma x_i \Sigma y_i}{n}\right]^2}{\left[\Sigma x_i^2 - \frac{(\Sigma x_i)^2}{n}\right]\left[\Sigma y_i^2 - \frac{(\Sigma y_i)^2}{n}\right]}$$

$\sigma_c = 59.00$

$m = 5.2$

$r^2 = 0.93$

APPENDIX 4

DETERMINATION OF MATERIAL CONSTANTS FOR HOEK AND BROWN'S EMPIRICAL EQUATION, USING MULTIPLE FAILURE STATE TEST RESULTS

$$\sigma_1 = \sigma_3 + \sqrt{m\,\sigma_c \cdot \sigma_3 + s\,\sigma_c^2}$$

FOR BROKEN ROCK

x_i	y_i	$x_i y_i$	x_i^2	y_i^2
0	45	0	0	2025
6.9	3014	20797	48	9084196
13.8	5975	82455	190	35700625
20.7	8968	185638	429	80425024
27.6	11257	310693	762	126720049
34.5	12723	438944	1190	161874729
Σ 103.5	41982	1038527	2619	413806648
Σ^2 10712	1762488324			

$y = (\sigma_1 - \sigma_3)^2 \quad x = \sigma_3 \quad n = 6$

σ_c to be used = intact rock = 59 MPa

$$m = \frac{1}{\sigma_c}\left[\frac{\Sigma x_i y_i - \frac{\Sigma x_i \Sigma y_i}{n}}{\Sigma x_i^2 - \frac{(\Sigma x_i)^2}{n}}\right]$$

$$s = \frac{1}{\sigma_c^2}\left[\frac{\Sigma y_i}{n} - m\,\sigma_c \frac{\Sigma x_i}{n}\right]$$

$$r^2 = \frac{\left[\Sigma x_i y_i - \frac{\Sigma x_i \Sigma y_i}{n}\right]^2}{\left[\Sigma x_i^2 - \frac{(\Sigma x_i)^2}{n}\right]\left[\Sigma y_i^2 - \frac{(\Sigma y_i)^2}{n}\right]}$$

$m = 6.4$

$r^2 = 0.99$

$s = 0.14$